

Superfast collective motion of magnetic particles

Olga Baun,¹ Peter Blümner,^{1,*} Friederike Schmid,¹ Evgeny S. Asmolov,^{2,3} and Olga I. Vinogradova^{2,4,5,†}

¹*Institut für Physik, Johannes Gutenberg-Universität Mainz, 55099 Mainz, Germany*

²*A.N. Frumkin Institute of Physical Chemistry and Electrochemistry,*

Russian Academy of Sciences, 31 Leninsky Prospect, 119071 Moscow, Russia

³*Institute of Mechanics, M.V. Lomonosov Moscow State University, 119991 Moscow, Russia*

⁴*Department of Physics, M.V. Lomonosov Moscow State University, 119991 Moscow, Russia*

⁵*DWI - Leibniz Institute for Interactive Materials, Forckenbeckstraße 50, 52056 Aachen, Germany*

(Dated: February 18, 2019)

It is well-known that magnetic forces can induce a formation of densely packed strings of magnetic particles or even sheafs of several strings (spindles). Here we show that in a sufficiently strong magnetic field, more complex aggregates of particles, translating with a much faster speed than would be for a single particle or even a spindle, can be assembled at the water-air interface. Such a superfast flotilla is composed of many distant strings or spindles, playing a role of its vessels, and moves, practically, as a whole. We provide theoretical results to interpret the effect of a collective motion of such magnetic vessels. Our theory shows that, in contrast to an isolated chain or spindle, which velocity grows logarithmically with the number of magnetic particles, the speed of the interface flotilla becomes much higher, being proportional to the square root of their number. These results may guide the design of magnetic systems for extremely fast controlled delivery.

I. INTRODUCTION

Magnetic micro- and nanoparticles have received much attention in recent years. They are important for a variety of promising applications including data storage, targeted drug delivery and cancer diagnostics/treatment systems [1, 2]. Most recent work has focused on the synthesis and biomedical modifications of the particles [1] or their detection and separation [3, 4]. Their field-directed assembly from dispersions to aggregates has also been studied for many years [5–10]. In typical applications, a magnetic field is applied, which does not change dramatically on the length scale of the aggregates. Hence, the magnetic moments of neighboring particles point in the same direction and exert dipolar forces upon each other, causing the formation of strings along the flux lines (see Fig. 1 (a)). This is analogous to the behavior of iron filings in classical demonstration experiments. If such strings are allowed to grow further until they reach a critical average length [11, 12], they form spindle-like aggregates (see Fig. 1 (b)), which at a certain size exert a repelling force on the neighboring string or spindle again, analogous to the familiar picture of iron filings in magnetic fields. Apart from inducing aggregation, time-dependent (e.g., rotating) magnetic fields and magnetic field gradients can also be used to manipulate and drive isolated particles [13, 14] and their aggregates [15–19].

The body of work investigating motion of particles in magnetic fields still remains rather scarce, although there has been some interest in recent years in questions surrounding the dynamic behavior of magnetic particles in microfluidic channels and at the liquid-air or solid-liquid

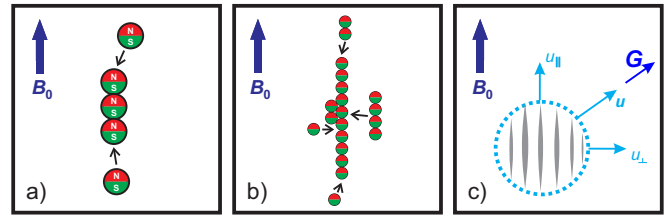


FIG. 1. Schematic presentation of particle aggregation: a) particles orient along the external homogeneous magnetic field, \mathbf{B} , and form strings by mutual dipolar attraction. b) Once a certain length is reached [11], particles or smaller particle chains can also attach towards the center of the string to form spindles. c) Strings and spindles can form larger assemblies (indicated by the circle and referred to as flotilla). The flotilla moves as a whole when a field gradient \mathbf{G} is applied with a velocity u . Due to the fact that the chains always align parallel to \mathbf{B}_0 the velocity is anisotropic with components u_{\parallel} and u_{\perp} .

interface. Questions of interest included the translation of isolated particles [20], the controlled motion of chains at the periodically rough solid [18], the propulsion of colloidal microworms [19], the formation of dynamic patterns on a fluid surface [16]. Most of the studies calculate the translational velocity by balancing the magnetic force on a single particle and the Stokes drag [5, 7, 11, 12, 15]. In other words, it is normally assumed that the motion of a particle is unaffected by the presence of other particles. However, recent experiment [21] has demonstrated that magnetic particles suspended at the fluid interface can move much faster than one would expect for an isolated particle, but these results have not been interpreted, and the understanding of such a superfast motion is still challenging. Clearly, in order to rationalize the situation, new experimental data and fresh theoretical concepts are necessary.

* Corresponding author: bluemner@uni-mainz.de

† Corresponding author: oivinograd@yahoo.com

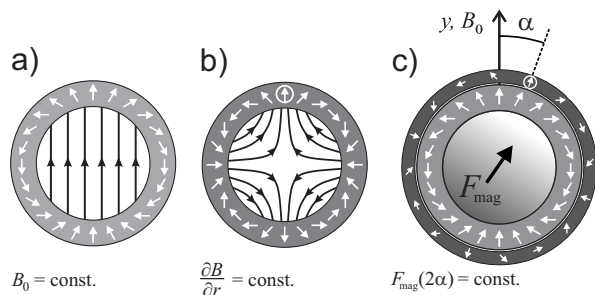


FIG. 2. Schematic drawing of a cross-section through a) an ideal Halbach dipole cylinder providing a homogeneous magnetic field, \mathbf{B}_0 ; b) an ideal Halbach quadrupole generating a constant radial magnetic field gradient. c) If the two are superimposed, only the gradient component along \mathbf{B}_0 is relevant to generate a magnetic force, \mathbf{F} , on particles in the inner volume. The angle of \mathbf{F} changes by 2α if the quadrupole is rotated by α relative to the dipole.

In this paper, we explore experimentally the fast motion of superpara/magnetic particles suspended at the water-air interface and suggest simple theoretical models describing the data. Our results show that strings or their clusters (spindles) form, but then assemble in a more complex aggregate referred to as a flotilla, where many distant chains or spindles, playing a role of vessels, move together practically as a whole (see Fig. 1(c)). The velocity of such a flotilla is orders of magnitude higher than that of a single particle, and is even much faster than for an isolated vessel. Our simple models describe well the velocities of isolated vessels and flotillas, relating them to the size of the aggregates, the parameters of constituting particles and their number. The formation of a fast flotilla of magnetic particles could greatly reduce the time required for controlled particle manipulations. This may have important consequences for controlled delivery of magnetic particles in various biomedical and other applications.

II. EXPERIMENTAL

The experiments were carried out using the same technique as in a recent study by two of us [21]. Its basic idea is to use a magnet system which provides a strong, homogeneous, dipolar magnetic field (\mathbf{B}_0) (cf. Fig. 2(a)) to magnetize and orient the superparamagnetic particles (SPPs) (as shown in Fig. 1), and a second quadrupolar field with a spatially constant tensor $\nabla\mathbf{B}$, superimposed on the first, to generate a magnetic force on the oriented particles (see Fig. 2(b)). In this configuration the motion of the particles is driven predominantly by the gradient \mathbf{G} of the field component in the direction of the homogeneous field, $\mathbf{G} = \nabla(\mathbf{B} \cdot \mathbf{B}_0)/B_0$. As a result, particles are guided with constant force and in a single direction over the entire inner volume of the magnet. The direction of the force is simply adjusted by varying the angle between



FIG. 3. Photograph of the experimental device: 1) Halbach dipole, 2) Halbach quadrupole (can be rotated), 3) Opening with Petri-dish, 4) stereo-microscope, 5) CCD-camera, 6) incident lightning on each side

the quadrupole and the dipole (see Fig. 2(c)). Since a single magnetic field gradient is forbidden by Gauss' law (the tensor $\nabla\mathbf{B}$ must be traceless), the other gradient component of the quadrupole determines the angular deviation of the force, which is negligible for $|\mathbf{B}_0| \gg |\mathbf{G}|r$. A possible realization of this idea is a coaxial arrangement of two Halbach cylinders [22, 23]. A Halbach dipole to evenly magnetize and orient the particles, and a Halbach quadrupole to generate the magnetic force, \mathbf{F} , on the SPPs.

The magnet system used is shown in Fig. 3. Design and characterization of this magnet system is described in detail in [21]. This system has an inner opening of 130 mm in diameter in which a Petri-dish (70 mm in diameter and 20 mm height) was centered. All experiments were done in the central area of this dish (ca. 40 mm in diameter), where the magnetic field has the following properties: $B_0 = 0.103(2)$ T and $G = 0.19(2)$ T/m. The Petri-dish was filled with ca. 30 ml of deionized water ($\mu = 0.9$ mPs).

To understand how the speed of the aggregate depends on the total number of constituent magnetic particles, which is determined optically, particles must be micron-sized. Here we use a commercial (micromod Partikeltechnologie GmbH, Rostock, Germany) sample of spherical magnetite (ca. 40% w/w) particles in a matrix of poly(D,L-lactic acid) with a molecular weight of 17 kD and a plain surface (product name: PLA-M 30 μm and product number: 12-00-304) with a size distribution range: 20-50 μm , centered at 30 μm ; magnetization $M = 4.3$ Am²/kg particles for $B = 0.1$ T; saturation magnetization $M > 6.6$ Am²/kg particles for $B > 1$ T; density: 1300 kg/m³, delivered as an aqueous suspension with 5.5×10^5 particles/ml).

From the stirred suspension 10 μl were extracted and injected into the Petri-dish using an Eppendorf pipette (Wetzlar, Germany). However, not all of the (theoretically expected) 5500 particles in this volume could be transferred into the water inside the dish because several stuck to the pipette, additionally some directly sunk to the ground. Smaller concentrations or volumes were

found to be unpractical because too many particles stuck at the pipette tip. In order to obtain aggregates formed by a certain number (order of magnitude) of particles, some of the strings were removed again from the sample by sucking them into another clean pipette. We note that the particles and particle aggregates studied here (those that did not sink to the ground) are confined at the air/water interface, hence the systems are effectively two dimensional.

The composition of the aggregates was studied using a stereo microscope (Motic SMZ-168, Wetzlar, Germany) with a modest magnification ($15\times$ to $100\times$) and incident illumination. The third tube of the microscope was equipped with a CCD-camera (moticom 1000, motic, Wetzlar, Germany) allowing to take snapshots as well as real-time videos. Once an aggregate of suitable size was formed and singled out, the number of particles, n , it is composed of was determined via the microscope. For smaller numbers ($n \lesssim 300$) this could be done at relative high magnifications where single particles could be identified. The composition of larger structures had to be estimated from graphical integrals of their shapes, which of course increased the error for larger n . The selected aggregate is then moved parallel and perpendicular to B_0 by rotating the quadrupole in steps of 45° (hence the forward and the particle movement happens in steps of 90°). In the lowest magnification the microscope has a field of view of $4 \times 4 \text{ mm}^2$ which is too small to study the typical velocities of the aggregates (except for very small n). Therefore, a digital camera (Fujifilm FinePix HS30EXR) was used to take real-time movies of this motion. A transparent foil with a millimeter-grid was attached to the bottom of the Petri-dish as a spatial reference. Particle and aggregate velocities were obtained from these videos using the image processing software Avidemux V5 (NCH Software, Greenwood Village CO, USA).

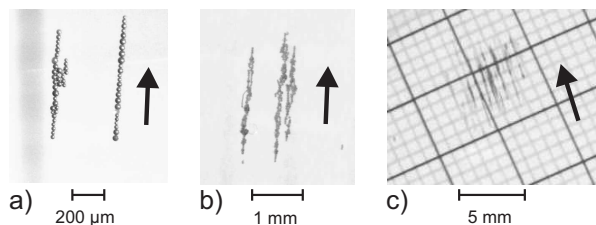


FIG. 4. Snapshots of typical aggregates from different amounts of $30 \mu\text{m}$ magnetite particles: a) typical vessel formation ($n \lesssim 100$). The assembly on the right is a string, while on left side already some particles attach close to the center (spindle). b) spindle-shaped vessels for larger n and c) a "flotilla" of such vessels. The black arrows indicate the direction of the homogeneous magnetic field B_0 .

III. RESULTS AND DISCUSSION

Shortly after the injection of the particles, strings and later spindles form from the initial cloud of particles (see Fig. 4). The aggregation occurs quasi instantly, but note that for nanoparticles it could take several minutes. After that several parallel distant vessels form a flotilla. As explained in the introduction, the reorganization of the initially dispersed particles into vessels (strings or spindles) is driven by magnetic dipolar interactions. The mechanism that keeps the flotilla together is less clear. Whereas the magnetic long-range interactions between parallel rigid strings made of identical dipolar particles are repulsive, fluctuations in flexible chains may induce long-range attractive interactions *via* a mechanism that was first pointed out by Halsey and Toor [24]. However, this mechanism would typically induce chain coalescence [6] and not stabilize larger arrays, i.e. flotillas, of well-separated vessels. Other possible sources of attraction are chain defects [5] or long-range capillary interactions mediated by the water-air interface [25, 26].

The aggregates can be set in motion by applying an additional (quadrupolar) field with constant gradient G as explained in Sec. II. The stationary velocities of the aggregates are found to be orders of magnitude higher than the velocities calculated for isolated particles. To study this effect more systematically, we have conducted experiments by translating aggregates containing different amounts of SPPs parallel and perpendicular to the direction of B_0 .

Table I shows the results of the velocity measurements of various aggregates which are then plotted in Fig. 5 as a function of the total number of particles (note that here we present data only for relatively small aggregates since it is difficult to count n in larger flotillas, which move even faster). The central observation can be summarized as follows: Under an applied magnetic force, particles forming a flotilla of vessels collectively translate at a much higher speed than one would expect for isolated particles. Why does this happen and what does this mean?

The detailed transport equations are rather complex, and it is difficult to extract a simple message from them. Our aim is more modest. We want to highlight the basic principles of observed phenomena in very compact terms. We model single isolated vessels by cylinders of radius a and length $2b$, which lie in the air-water interface and translate under the action of a tangent to this interface external magnetic force F_n . We consider the hydrodynamic drag caused by the water phase and neglect the friction with the air phase. Due to the small sizes of the aggregates and their relatively small velocities (of the order of mm/s), the Reynolds number is small, so that we use Stokes equations. We further assume that the air-water interface is strictly planar and that the floating at the interface particles are half immersed in water. Physically, this means that we neglect differences of the surface tension of the particles with water or air and gravitational forces. With these assumptions, the solution of

TABLE I. Experimentally determined properties of PLA-M SPPs: n is the total number of particles in the aggregate, N is the number of vessels per flotilla with n_i as the number of particles in its individual vessel. The velocities parallel, u_{\parallel} , and perpendicular, u_{\perp} , to \mathbf{B}_0 were determined for each aggregate as described in Sec. II. The same data are plotted in Fig. 5.

n	$n_i (i = 1..N)$	u_{\parallel} [mm/s]	u_{\perp} [mm/s]
3	$n_1 = 3$	0.25 ± 0.01	0 ± 0.06
51 ± 1	$n_1 = 51 \pm 1$	0.96 ± 0.1	0.74 ± 0.06
105 ± 15	$n_1 = 105 \pm 15$	1.13 ± 0.1	0.71 ± 0.06
273 ± 60	$n_1 = 12 \pm 25$ $n_2 = 150 \pm 35$	1.25 ± 0.1	0.79 ± 0.07
287 ± 60	$n_1 = 102 \pm 25$ $n_2 = 105 \pm 25$ $n_3 = 80 \pm 10$	1.25 ± 0.11	0.78 ± 0.07
499 ± 65	$n_1 = 181 \pm 25$ $n_2 = 191 \pm 25$ $n_3 = 127 \pm 15$	1.5 ± 0.11	0.86 ± 0.07
742 ± 125	$n_1 = 230 \pm 25$ $n_2 = 512 \pm 100$	1.76 ± 0.1	1.44 ± 0.07
1350 ± 165	$n_1 = 450 \pm 50$ $n_2 = 400 \pm 50$ $n_3 = 350 \pm 40$ $n_4 = 150 \pm 25$	2.64 ± 0.2	1.26 ± 0.07

the Stokes equation for the hydrodynamic flows in the half space underneath the aggregates can be obtained from the solution for a fully immersed aggregate by simply “cutting away” the upper half space. Hence we can use the available results for the resistance of bodies in an infinitely extended fluid at low Reynolds numbers [27] after replacing the viscosity of water, μ by the effective viscosity $\mu_{\text{eff}} = \mu/2$ [28].

In the limit of very long and thin cylinders, $b \gg a$, the translational velocity in longitudinal and transverse direction (parallel and perpendicular to the string orientation, i.e. \mathbf{B}_0), u_{\parallel} and u_{\perp} , can be expressed as (Eqs. (5-11.52) and (5-11.54) in Ref. 27),

$$u_{\parallel} \approx \frac{F_n [\ln(2b/a) - 0.72]}{4\pi\mu_{\text{eff}}b}. \quad (1)$$

$$u_{\perp} \approx \frac{F_n [\ln(2b/a) + 1/2]}{8\pi\mu_{\text{eff}}b}. \quad (2)$$

For a single string we naturally set the cylinder radius a as equal to the particle radius and, therefore, we have $b = na$, where n is the number of magnetic particles in a single vessel. The force acting on the single vessel can be calculated as $F_n = n|\mathbf{f}|$, where \mathbf{f} is the magnetic force acting on a single particle. The latter can be expressed as $\mathbf{f} = \nabla(\mathbf{m} \cdot \mathbf{B})$, where the vector \mathbf{m} is the magnetic moment which is aligned along \mathbf{B}_0 in this case, $\mathbf{m} = \frac{4}{3}\pi a^3 \rho M(B)\mathbf{B}_0/B_0$; ρ is the density and $M(B)$ the magnetization (which typically is constant over space, because $B = B_0$ is homogeneous as G only causes a small deviation on the lengthscale of the aggregates).

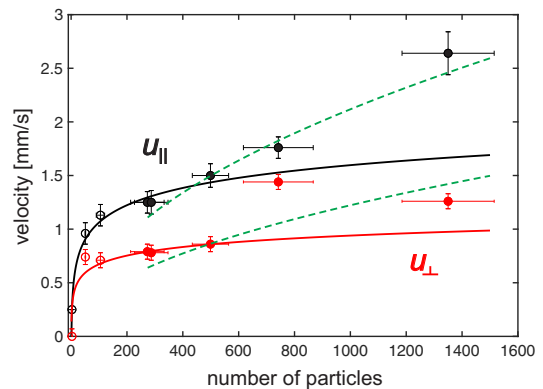


FIG. 5. Experimentally obtained longitudinal (u_{\parallel} in black) and transverse (u_{\perp} in red) velocities of vessels and flotillas vs the number of constituent particles, n . The open circles correspond to single vessels while the solid circles correspond to flotillas of 2 - 4 strings each (c. f. Table I). The solid lines represent fits of Eq.(3) (in black) and Eq. (4) (in red) to the data, where the radius of the particles was fitted for both curves as $a = 17.4\mu\text{m} \pm 0.6\mu\text{m}$ while the other parameters in Eq. (5) were taken from Sec. II. The dashed green lines show the prediction of Eq. (6) for flotillas only. Here, ϕ was adjusted to cover the range of data. The lower curve corresponds to $\phi = 0.02$ and the upper to $\phi = 0.06$. See text for more details.

Hence, the force on a single particle can be simplified as $|\mathbf{f}| = \frac{4}{3}\pi a^3 \rho M G$. By substituting the expression for F_n in Eqs.(1) and (2) we obtain

$$u_{\parallel} \approx 2C [\ln(2n) - 0.72] \quad (3)$$

$$u_{\perp} \approx C [\ln(2n) + 0.5] \quad (4)$$

$$\text{with } C = a^2 \rho M G / 6\mu_{\text{eff}}. \quad (5)$$

The important conclusion from Eqs.(3) and (4) is that both u_{\parallel} and u_{\perp} grow logarithmically with n . When the force is applied at some angle α to the cylinder axis (the \mathbf{B}_0 - or y -axis) its velocity will be $\mathbf{u} = u_{\perp} \mathbf{e}_x \sin \alpha + u_{\parallel} \mathbf{e}_y \cos \alpha$. Therefore, the velocity of a vessel (here a string) in any direction scales as $\ln(n)$ at large n . This suggests that it should be impossible to obtain ultrafast velocities just by increasing the number of particles in a single vessel.

Fig. 5 shows a comparison of the experimental data (symbols) with the theoretical predictions of Eqs. (3) and (4) represented by solid lines. The solid symbols represent aggregates which consists of more than one string. All data were fitted with Eqs.(3) and (4) using the parameters given in Sec. II except for the radius. This seemed to be appropriate since the particles showed quite some dispersion. The fit yielded $a = 17.4\mu\text{m} \pm 0.6\mu\text{m}$, which is within the expected range. Up to particle numbers of about 500 the fit is quite good, confirming the validity of our simple model. For higher values $n > 500$, the experimental velocities are significantly larger than the theoretical prediction. Whereas small aggregates (with 100 particles or less) consist of single vessels only, these larger flotillas contain several

vessels (up to four at $n \approx 1400$).

We next calculate the velocity of a large flotilla, assuming that its strings and fluid between them move with the same speed. Strictly speaking, this assumption is valid for close particle packing only, but for smaller area fraction of solids ϕ we should take into account hydrodynamic interactions between strings to evaluate their speed more accurately. In our simple theory a collective vessel translation is modeled by the motion of a disc (which is the limiting case of an oblate spheroid) under the force perpendicular to the axis of rotation. According to Ref. 27, Eq. (5-11.25), for a thin disk of radius R its velocity is given by $u \approx 3F_{nN}/32R\mu_{\text{eff}}$, provided $a \ll R$. In our case, the disk radius can be approximated as $R \approx a(nN/\phi)^{1/2}$ where N is the number of vessels. For a given ϕ , and using $F_{nN} = nN|\mathbf{f}|$, we obtain

$$u = C \frac{3}{4} \pi \sqrt{nN\phi} \quad (6)$$

with C defined as above (Eq. (5)). Hence the disk velocity scales as $n^{1/2}$, i.e., it grows much faster with n than in the case of single strings. Even more importantly, the flotilla consists of N vessels, which further increases its speed compared to isolated vessels.

We recall that the data in Fig. 5 indicate that in the flotilla regime the particle transport is anisotropic, and the speed of flotillas is highest in the longitudinal (i.e. parallel to \mathbf{B}_0) direction. However, Eq. (6), which oversimplifies hydrodynamic interactions between vessels, obviously predicts an isotropic behavior. We also note that the shape of flotillas is often elliptical, rather than circular (see Fig. 4). Nevertheless, Eq. (6) provides an explanation of a much higher speed of the flotillas compared to isolated vessels. Indeed, the two green dashed curves included in Fig. 5 plot the predictions of Eq. (6) for two values of the solid area fraction, ϕ , $\phi = 0.02$ (lower curve) and $\phi = 0.06$ (upper curve), and we see that theoretical results agree well with the experimental data. Attempts to estimate ϕ experimentally turned out difficult due to the variable shapes of the flotillas. Forcing a circular shape gave the estimate $\phi < 0.1$, however with an error of the same size. Thus, the consideration above is quite approximate, but it provides us with some guidance.

Finally we note that in all cases considered here (Eqs. (3), (4), Eq. (6)), the velocity scales like $u \propto C \propto a^2$ with the particle size, due to the fact that the magnetic force on the disk is proportional to its volume while the drag is proportional to its radius. Specifically, the disc velocity for total particle volume $V = 4\pi a^3 nN/3$ can be written as

$$u = \frac{\rho MG(3\pi aV\phi)^{1/2}}{16\mu_{\text{eff}}}. \quad (7)$$

Since $u \propto a^{1/2}$, the collective velocity of vessels moving in a disk/flotilla should be larger for bigger particles.

IV. CONCLUSION

To summarize, we have shown that magnetic particles can be manipulated and steered very efficiently by magnetic fields using our setup of combined strong dipolar and weak quadrupolar magnetic fields, much more efficiently than one would expect based on the Stokes friction of single particles. The reason is that the dipolar field induces particle orientation and subsequent aggregation, and that these aggregates then move as a whole. The aggregates are hierarchically organized with strings or spindles (vessels) being the lowest level entities, which are further organized in flotillas. The packing of particles in vessels already leads to their high translational speed in the presence of a steering field. However, the formation of flotillas of many vessels further and dramatically increases the velocity response of particles to the steering field.

We have provided a theoretical interpretation of our data, and found good agreement between our model and experiment. Our theoretical model predicts that the velocity of vessels at fixed number of constituent particles n should scale as $\ln(n)$, whereas the velocity of disks increases with \sqrt{n} . This explains why disks are much faster at large n .

In the situation considered in the present work, the particles were located at water-air interface, so that the shape of the flotillas was two-dimensional (disks). Preliminary results in bulk solutions suggest that a three-dimensional association of vessels is also possible (unpublished). An association into sphere-shaped flotillas should speed up the particles even further. In that case the velocity of the fully immersed in water sphere of radius $R = a(nN/\varphi)^{1/3}$, where φ is the volume fraction of solids, would scale as $N^{2/3}$ following

$$u = \frac{F_{nN}}{6\pi R\mu} = \frac{2a^2 \rho MG(nN)^{2/3} \varphi^{1/3}}{9\mu}. \quad (8)$$

For given total particle volume V and particle volume fraction φ , the velocity then becomes independent of particle size:

$$u = \frac{2\rho MG(3V/4\pi)^{2/3} \varphi^{1/3}}{9\mu}. \quad (9)$$

Thus superfast transport can be achieved for particles of any size in this case.

The remaining open question is why the flotillas form at all. In Monte Carlo simulation of monodisperse, purely repulsive, dipolar particles, no such association was observed (unpublished data). As mentioned in the main text, chain defects may provide a possible explanation. Such defects could be induced, e.g., by the polydispersity of particles. Alternatively, the flotillas may be stabilized by elastic interactions due to deformations of the air-water interface. This interaction mechanism would however be restricted to particles at interfaces. As we have shown, the association of magnetic particles to flotillas

highly enhances their response to external steering fields, and they can thus be manipulated much more efficiently. In future work, we thus plan to identify and investigate possible association mechanisms in order to be able to control and exploit them.

ACKNOWLEDGMENTS

This work was funded by the German Research Foundation (DFG), SFB 1066, within projects A3, B5 and

Q1. PB and OB wish to acknowledge additional funding by a grant of the Johannes Gutenberg University Mainz (Inneruniversitäre Forschungsförderung). ESA and OIV acknowledge support of the Russian Ministry of Education and Science.

-
- [1] S. Singamaneni, V. N. Bliznyuk, C. Binek, and E. Y. Tsymbal, *J. Mater. Chem.* **21**, 16819 (2011).
- [2] P. Tierno, *Phys. Chem. Chem. Phys.* **16**, 23515 (2014).
- [3] M. Zborowski, L. Sun, L. R. Moore, P. S. Williams, and J. J. Chalmers, *J. Magn. Magn. Mater.* **194**, 224 (1999).
- [4] N. Pamme, J. C. T. Eijkel, and A. Manz, *J. Magn. Magn. Mater.* **307**, 237 (2006).
- [5] J. E. Martin, K. M. Hill, and C. P. Tigges, *Phys. Rev. E* **59**, 5676 (1999).
- [6] E. M. Furst and A. P. Gast, *Phys. Rev. E* **62**, 6916 (2000).
- [7] Y. Lalatonne, J. Richardi, and M. P. Pileni, *Nature Materials* **3**, 121 (2004).
- [8] S. M. Taheri, M. Michaelis, T. Friedrich, B. Forster, M. Drechsler, F. M. Romer, P. Bosecke, T. Narayanan, B. Weber, I. Rehberg, S. Rosenfeldt, and S. Forster, *PNAS* **112**, 14484 (2015).
- [9] Y.-H. Li, T.-Y. Su, T.-L. Chang, and Y.-W. Lee, *Microelectronic Engineering* **153**, 37 (2016).
- [10] S. H. L. Klapp, *Curr. Opin. in Coll. Interf. Sci.* **21**, 76 (2016).
- [11] D. Heinrich, A. R. Goni, A. Smessaert, S. H. L. Klapp, L. M. C. Cerioni, T. M. Osan, D. J. Pusiol, and C. Thomsen, *Phys. Rev. Lett.* **106**, 208301 (2011).
- [12] D. Heinrich, A. R. Goni, T. M. Osan, L. M. C. Cerioni, A. Smessaert, S. H. L. Klapp, J. Faraudo, D. J. Pusiol, and C. Thomsen, *Soft Matter* **11**, 7606 (2015).
- [13] L. Wu, Y. Zhang, M. Palaniapan, and P. Roy, *J. Appl. Phys.* **105**, 123909 (2009).
- [14] R. Zhou, F. Bai, and C. Wang, *Lab on a Chip* **17**, 401 (2017).
- [15] S. Melle and J. E. Martin, *J. Chem. Phys.* **118**, 9875 (2003).
- [16] M. Belkin, A. Snezhko, I. S. Aranson, and W. K. Kwok, *Phys. Rev. Lett.* **99**, 158301 (2007).
- [17] J. E. Martin and A. Snezhko, *Rep. Prog. Phys.* **76**, 126601 (2013).
- [18] A. V. Straube and P. Tierno, *Soft Matter* **10**, 3915 (2014).
- [19] P. Martinez-Pedrero, A. Ortiz-Ambriz, I. Pagonabarraga, and P. Tierno, *Phys. Rev. Lett.* **115**, 138301 (2015).
- [20] S. S. Shevkoplyas, A. C. Siegel, R. M. Westervelt, M. G. Prentiss, and G. M. Whitesides, *Lab on a Chip* **7**, 1294 (2007).
- [21] O. Baun and P. Blümmler, *J. Magn. Magn. Mater.* **439**, 294 (2017).
- [22] K. Halbach, *Nucl. Instr. Methods* **169**, 1 (1980).
- [23] P. Blümmler and F. Casanova, in *Mobile NMR and MRI* (The Royal Society of Chemistry, Cambridge, UK, 2015) pp. 133–157.
- [24] T. C. Halsey and W. Toor, *J. Stat. Phys.* **61**, 1257 (1990).
- [25] A. Dominguez, M. Oettel, and S. Dietrich, *J. Chem. Phys.* **127**, 204706 (2007).
- [26] F. Bresme and M. Oettel, *J. Phys.: Cond. Matter* **19**, 413101 (2007).
- [27] J. Happel and H. Brenner, *Low Reynolds number hydrodynamics: with special applications to particulate media* (Englewood Cliffs, NJ: Prentics Hall, 1965).
- [28] K. Ranger, *Int. J. Multiph. Flow* **4**, 263 (1978).